Supporting Information

Molecular-level control over plasmonic properties in silver nanoparticle/self-assembling peptide hybrids

Yin Wang,[1,2] Xiaozhou Yang,[1] Tianyu Liu,[1] Zhao Li,[1,2] David Leskauskas,[1] Guoliang Liu*,[1, 2] John B. Matson*[1, 2,]

[1]Department of Chemistry, and [2]Macromolecules Innovation Institute, Virginia Tech, Blacksburg, VA 24061, United States

*Correspondence: gliu1@vt.edu, jbmatson@vt.edu

Table of Contents

Materials:

All Fmoc amino acids and Rink amide MBHA resin were purchased from Peak Polypeptide Biosystems LLC (P3BioSystems, Louisville, KY, USA). 4-Formylbenzoic acid (FBA) was purchased from Chem-Impex International, Inc (Wood Dale, IL, USA). Thiobenzoic acid, silver nitrate, ascorbic acid (AA), poly(sodium 4-styrenesulfonate) (PSSS, $\overline{M}_w \approx 1000$ kDa), sodium citrate tribasic dihydrate, and sodium borohydride were purchased from Sigma-Aldrich (St. Louis, MO, USA). Rhodamine B (RhB) was purchased from Alfa Aesar (Tewksbury, MA, USA). All other reagents were sourced from Sigma-Aldrich (St. Louis, MO) or VWR (Radnor, PA, USA), unless otherwise stated. *S*-Benzoylthiohydroxylamine (SBTHA) was synthesized according to our previous report.[1] Ultrapure water was acquired from a Thermo Scientific Barnstead GenPure Pro with a resistivity of 16 MΩ. All glassware and stir bars used in this study were rinsed by freshly prepared aqua regia solution (HCl/HNO_3, molar ratio = 3:1) prior to use.

Peptide synthesis:

Peptides used in this study were manually synthesized using standard 9-fluorenylmethoxycarbonyl (Fmoc) solid phase synthesis techniques at a 0.5 mmol scale. Fmoc deprotection steps were carried out by treating the Rink amide MBHA resin with 4-methylpiperidine in *N*,*N*-dimethylformamide (DMF) (20% v/v). Amino acid coupling steps were performed following Fmoc deprotection by treating the resin with Fmoc-amino acid, *O*-benzotriazole-*N,N,N′,N′*-tetramethyluronium hexafluorophosphate (HBTU), and diisopropylethylamine (DIEA) (4:3.96:10 molar ratio to amine groups on resin) in DMF for 2 h. After coupling of the final amino acid, removal of the Mtt protecting group derived from Fmoc-Lys(Mtt)-OH was achieved by treating the resin with trifluoroacetic acid (TFA)/triisopropylsilane (TIS)/DCM (3:5:92). FBA was then coupled to the Lys ε-amine using the same coupling conditions as noted above for Fmoc amino acids. The final Fmoc group was then removed, and the *N*-terminus was acetylated by treating the resin with a mixture of acetic anhydride (10 mL, 20% in DMF) and DIEA (80 μL) three times. Finally, peptides were cleaved from the resin by treatment with a TFA/H_2O (97.5:2.5) solution (15 mL) for 3 h. The solution was concentrated *in vacuo* and triturated with cold diethyl ether to precipitate the crude peptide. Following centrifugation to remove the supernatant liquid, the crude materials were dissolved in the mixture of water and acetonitrile containing 0.1% NH_4OH (v/v) for purification.

Peptides were purified by preparative RP-HPLC using an Agilent Technologies 1260 Infinity HPLC system (Agilent Technologies, Santa Clara, CA) equipped with a fraction collector. Separations were performed using an Agilent PLRP-S column (100 Å, 10 μm, 150 × 25 mm) monitoring at 220 nm. The expected mass was confirmed using electrospray ionization-mass spectrometry (ESI-MS) (Advion ExpressIon Compact Mass Spectrometer). Fractions containing pure products were combined and lyophilized (FreeZone −105 °C, Labconco, Kansas City, MO), and then stored at −20 °C until needed.

Synthesis of aromatic peptide amphiphiles (APAs)

Both APAs were synthesized according to the previously published methods.[2] An example synthesis (**K_S*C'*EK_S**) is as follows: Lyophilized FBA-terminated peptide (50 mg, 58 μmol) and SBTHA (71 mg, 460 μmol) were dissolved in anhydrous DMSO (700 μL). TFA (10 μL) was added to catalyze the reaction. After standing for 4 h at rt, the solution was diluted with HPLC grade water and acetonitrile (8 mL in total, v/v = 1:1). The pH of the solution was adjusted to 7 by addition of aliquots of 0.1 g/mL aqueous NaOH before purification by preparative RP-HPLC. Product-containing fractions were combined and lyophilized to afford each compound as a white powder.

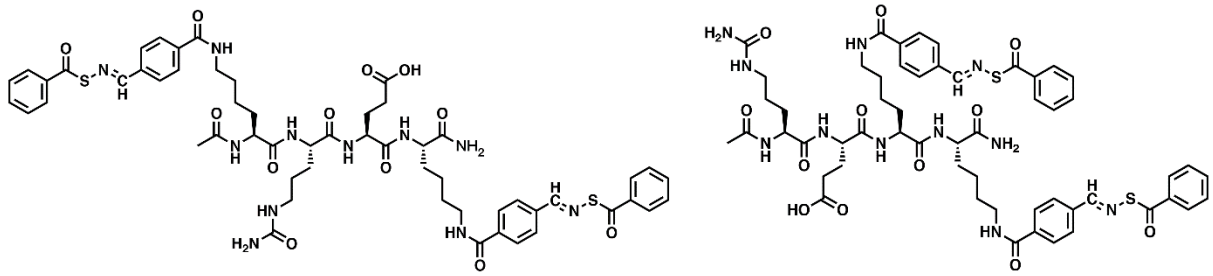

Figure S1. Molecular structures of APAs studied in this manuscript.

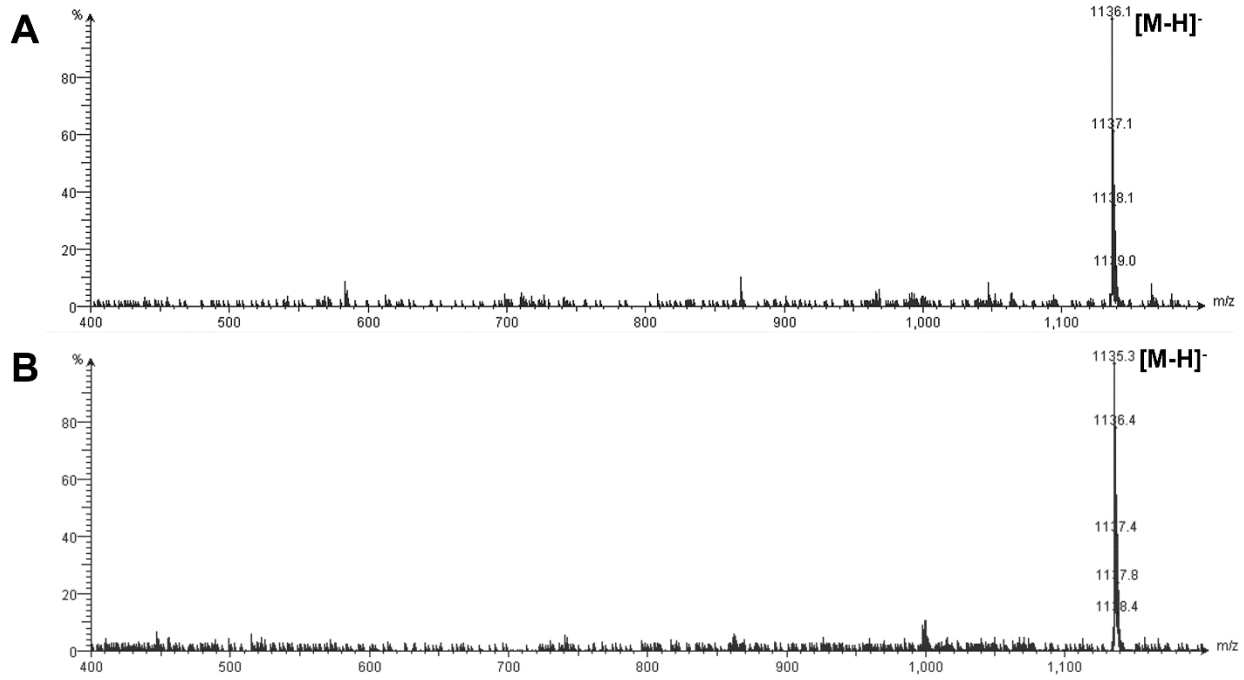

Figure S2. ESI mass spectra of (A) $\mathbf{K_S}\boldsymbol{C'}\mathbf{EK_S}$ and (B) $\boldsymbol{C'}\mathbf{EK_SK_S}$.

Characterization of self-assembled APAs

Conventional transmission electron microscopy (TEM):

1 mM stock solutions of APAs in 10 mM phosphate buffer (PB) solution (pH 7.4) were prepared by direct dissolution of the lyophilized powders. Samples were allowed to age overnight. An aliquot of each solution was removed immediately prior to TEM sample preparation and diluted with 10 mM PB to 100 μM. Next, 10 μL of this solution was deposited on a carbon-coated copper grid (Electron Microscopy Services, Hatfield, PA, USA) and allowed to stand for 5 min. Excess solution was wicked away by a small piece of filter paper, and then DI water was deposited, allowed to stand for 40 sec, and then wicked away to wash away excess salts. Finally, 10 μL of a 2 wt.% aqueous uranyl acetate (UA) solution was deposited on the grid for 5 min. A thin layer was generated after carefully wicking away excess UA. The sample grid was then allowed to dry at rt prior to imaging. Bright-field TEM imaging was performed on a Philips EM420 TEM operated at an acceleration voltage of 100 kV. TEM images were recorded by a slow scan CCD camera.

Circular dichroism (CD) spectroscopy:

CD spectra of APAs (190-400 nm) and Ag/APA hybrid complexes (350-580 nm) were recorded on a Jasco J-815 spectropolarimeter (JASCO, Easton, MD, USA) using a 1 mm or 2 mm path length quartz UV-Vis absorption cell (Thermo Fisher Scientific, Pittsburgh, PA, USA). For APA measurements, 100 μM samples were diluted from 1 mM stock solution in 10 mM phosphate buffer (pH=7.4) and used immediately. For Ag/APA hybrid complex measurements, samples were taken from scintillation vials and used without dilution (APA concentration was 6.3 μM and Ag^+ was 114 μM). A background spectrum of the solvent was acquired and subtracted from each sample spectrum. All measurements were conducted in triplicate.

Molecular packing within self-assembled APAs before and after addition of $AgNO_3$ and PSSS was assessed by circular dichroism (CD) spectroscopy. Before adding salts, both $\mathbf{K_S}\boldsymbol{C'}\mathbf{EK_S}$ and $\boldsymbol{C'}\mathbf{EK_SK_S}$ displayed a classical β-sheet secondary structure, along with a strong SATO absorption. Interestingly, the CD spectra were nearly identical mirror images; this inversion likely resulted from different handedness of the assemblies.[3-4] When $AgNO_3$ and PSSS were added to the solution, the spectrum changed into a random coil-like structure for $\mathbf{K_S}\boldsymbol{C'}\mathbf{EK_S}$ (the same as when only PSSS was added to the solution). However, the spectrum did not change significantly for $\boldsymbol{C'}\mathbf{EK_SK_S}$. These changes were consistent with TEM observations, where $\mathbf{K_S}\boldsymbol{C'}\mathbf{EK_S}$ showed significant morphological changes after salt addition, but $\boldsymbol{C'}\mathbf{EK_SK_S}$ did not.

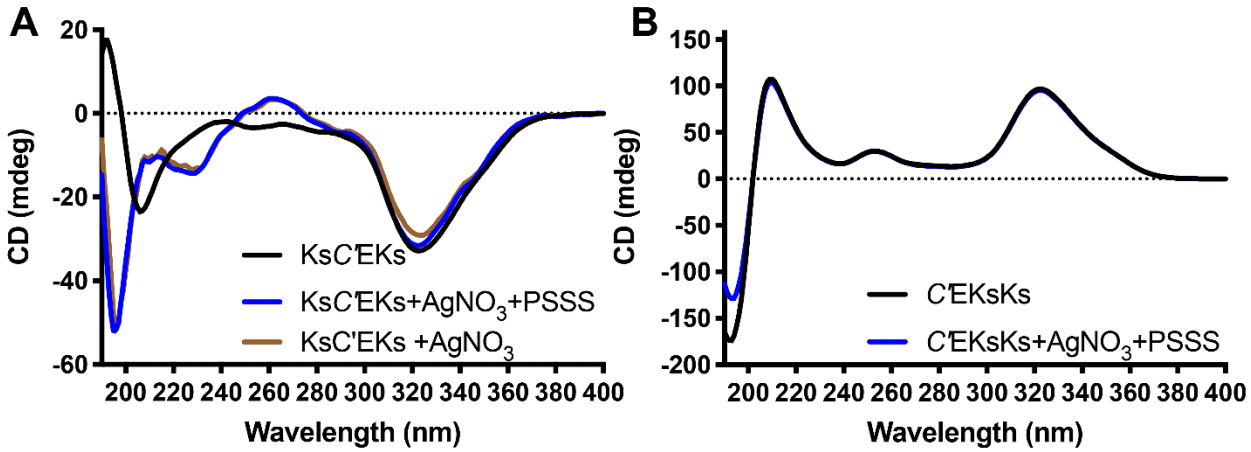

Figure S3. CD spectra of (A) $\mathbf{K_S}\boldsymbol{C'}\mathbf{EK_S}$ and (B) $\boldsymbol{C'}\mathbf{EK_SK_S}$ in 10 mM PB before and after adding $AgNO_3$ and PSSS.

UV-Vis spectroscopy:

UV-Vis spectra of APAs from 190 to 400 nm were also recorded on a Jasco J-815 spectropolarimeter (JASCO, Easton, MD, USA) using a 1 mm path length quartz UV-Vis absorption cell (Thermo Fisher Scientific, Pittsburgh, PA, USA). 100 μM samples were diluted from 1 mM stock solution in 10 mM phosphate buffer (pH=7.4) and analyzed immediately. A background spectrum of the solvent was acquired and subtracted from each sample spectrum.

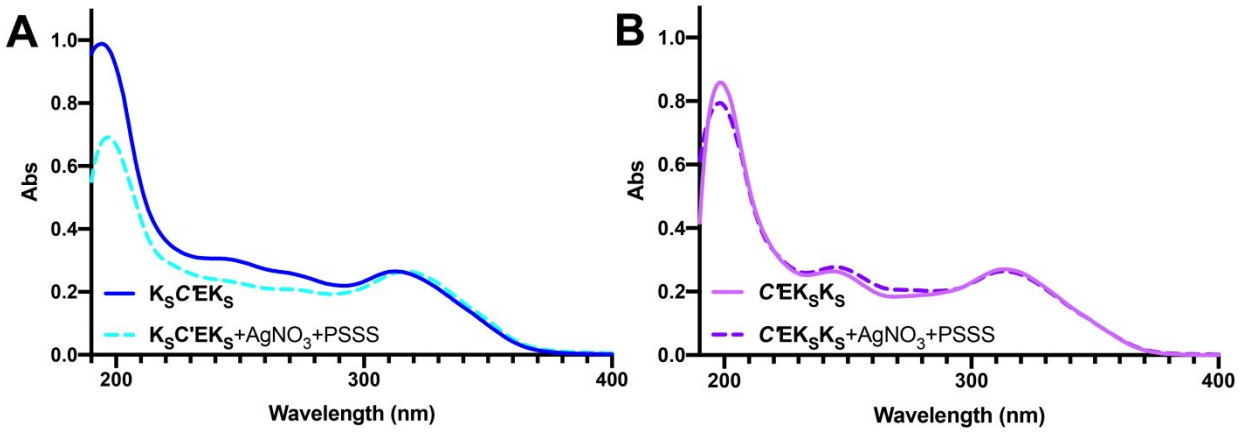

Figure S4. UV-Vis spectra of (A) $\mathbf{K_S}\boldsymbol{C'}\mathbf{EK_S}$ and (B) $\boldsymbol{C'}\mathbf{EK_SK_S}$ in 10 mM PB before and after adding1 mL $AgNO_3$ (0.5 mM in water) and 50 μL PSSS (0.5 mg mL^{-1} in water).

Effects on morphological changes by addition of $AgNO_3$ and PSSS

In general, addition of $AgNO_3$ and PSSS to APAs in solution can both induce salting-out by an excluded-volume mechanism[5] and screen the carboxylate groups of glutamic acid residues displayed on the surface of nanoribbons. This combination of effects influenced APAs $\mathbf{K_S}\boldsymbol{C'}\mathbf{EK_S}$ and $\boldsymbol{C'}\mathbf{EK_SK_S}$ differently—APA $\mathbf{K_S}\boldsymbol{C'}\mathbf{EK_S}$ transitioned from a nanoribbon to a nanohelix, while APA $\boldsymbol{C'}\mathbf{EK_SK_S}$ did not undergo a morphological transition. Based on the shifts in the UV-Vis spectra of both APAs above, we speculate that hydrophobic interactions among $\mathbf{K_S}\boldsymbol{C'}\mathbf{EK_S}$ molecules increased when $AgNO_3$ and PSSS were added to the solution, as indicated by a hypochromic shift in the absorbance maximum.[6-7] An increased hydrophobic interaction has been identified as a driving force for the formation of the nanohelices in other systems.[8-11] In contrast, the hydrophobic interactions among $\boldsymbol{C'}\mathbf{EK_SK_S}$ molecules did not change upon addition of salts, implying that addition of PSSS and $AgNO_3$ did not have a large impact on the molecular packing of this APA, consistent with TEM (Figure 1) and CD results (Figure S3).

Synthesis of Ag seeds on APAs (AgSD/APA):
In a 1-dram vial, 1 mL of $AgNO_3$ solution (0.5 mM in water) was mixed with 1 mL of pre-assembled APA solution (200 µM in 10 mM PB) for 45 min to facilitate adsorption of Ag^+ onto APA nanostructures. Next, 0.9 mL of Milli-Q water, 0.1 mL of sodium citrate solution (2.5 mM in water), and 50 µL of PSSS (0.5 mg mL^{-1} in water) were added to the $AgNO_3$/APA solution. Afterwards, 60 µL of $NaBH_4$ solution (10 mM in ice-cold water) was prepared and immediately added to the $AgNO_3$/APA solution. The solution was vortexed for 1 min. During vortexing, the solution color turned from colorless to brown, indicating the formation of small silver seeds (referred to as AgSD/APA).

Growth of Ag nanoparticles templated by APA (AgNP/APA) from AgSD/APA:
To a scintillation vial equipped with a stir bar, 10 µL of ascorbic acid solution (10 mM in water) and water (1.33 mL) were added. Subsequently, AgSD/APA solution (50-1000 µL) was added. Afterwards, 400 µL of $AgNO_3$ solution (0.5 mM in water) was added to the growth solution using a syringe pump at an injection rate of 0.133 mL min^{-1}. After complete addition, 0.1 mL of sodium citrate solution (2.5 mM in water) was added to cap and stabilize the AgNPs. The resulting suspension is referred to as AgNP/APA.

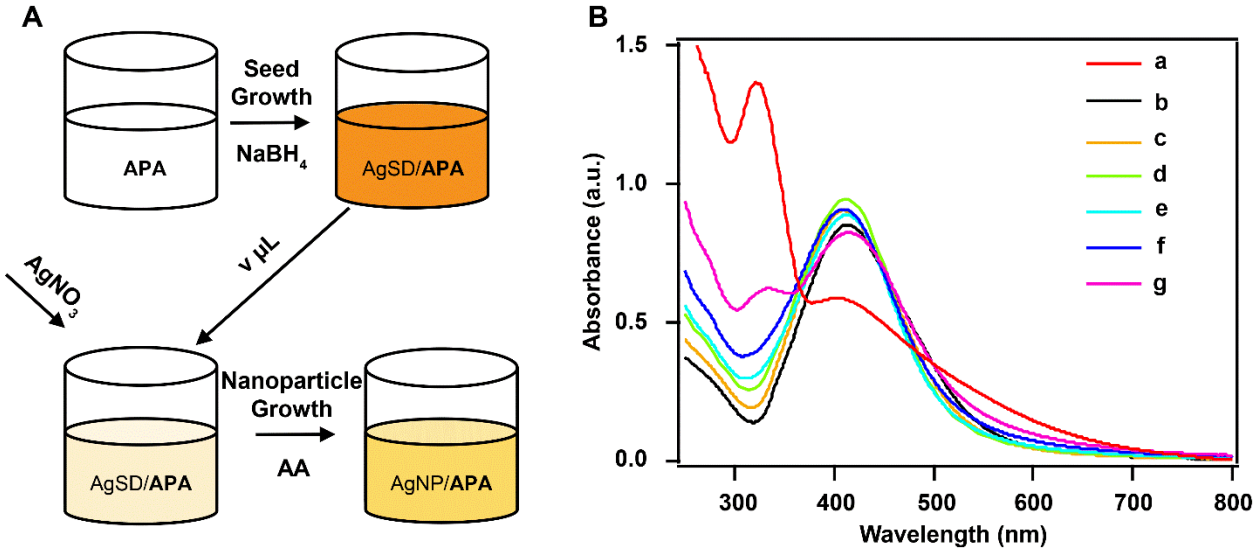

Figure S5. (A) Schematic illustration for preparation of AgNP/APA from AgSD/APA solutions. (B) UV-Vis spectra of (a) AgSD/$\mathbf{K_SC'EK_S}$ and (b-g) AgNP/$\mathbf{K_SC'EK_S}$ grew from (b) 50 µL, (c) 100 µL, (d) 200 µL, (e) 300 µL, (f) 500 µL, and (g) 1000 µL of AgSD/$\mathbf{K_SC'EK_S}$ solutions. The peaks near 320 nm and 400 nm correspond to the absorptions of SATO and AgNPs, respectively.

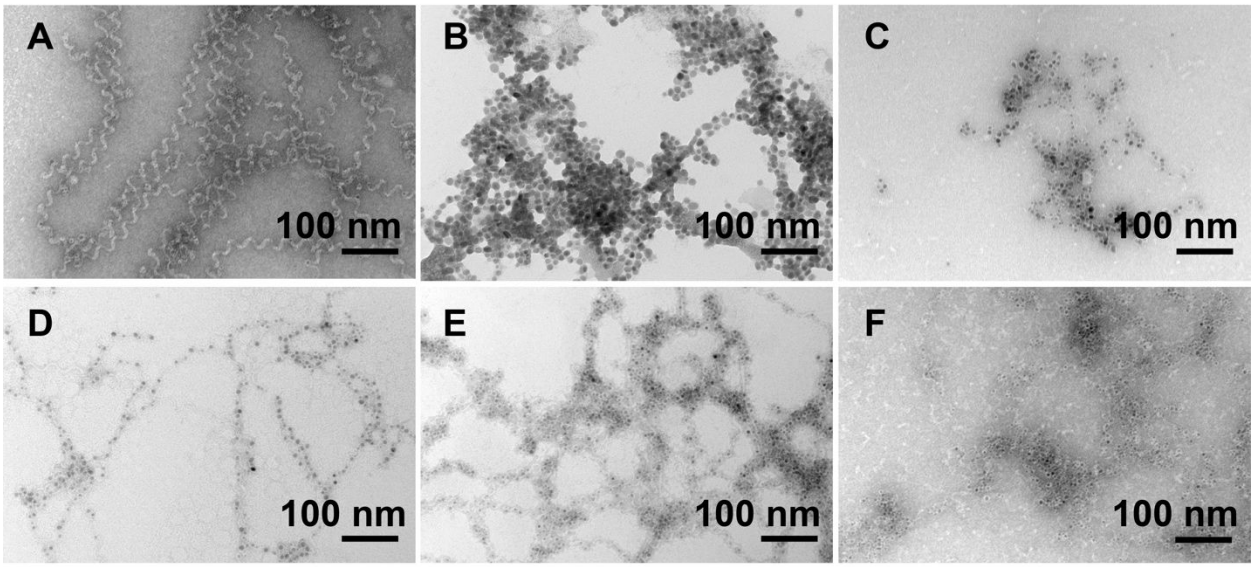

Figure S6. Representative TEM images of (A) AgSD/$\mathbf{K_S}\boldsymbol{C'}\mathbf{EK_S}$ and (B-F) AgNP/$\mathbf{K_S}\boldsymbol{C'}\mathbf{EK_S}$ grown from (B) 50 μL, (C) 100 μL, (D) 300 μL, (E) 500 μL, and (F) 1000 μL of AgSD/$\mathbf{K_S}\boldsymbol{C'}\mathbf{EK_S}$ solutions. When the volume of the seed solution used for the nanoparticle growth was below 200 μL (panels B and C), the morphology of nanohelices was not preserved.

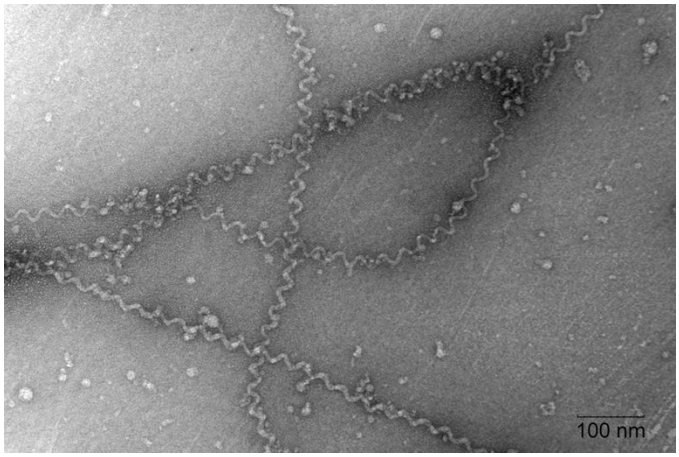

Figure S7. A representative TEM image of $\mathbf{K_S}\boldsymbol{C'}\mathbf{EK_S}$ nanohelices in the presence of $AgNO_3$ (without PSSS) before reduction by $NaBH_4$.

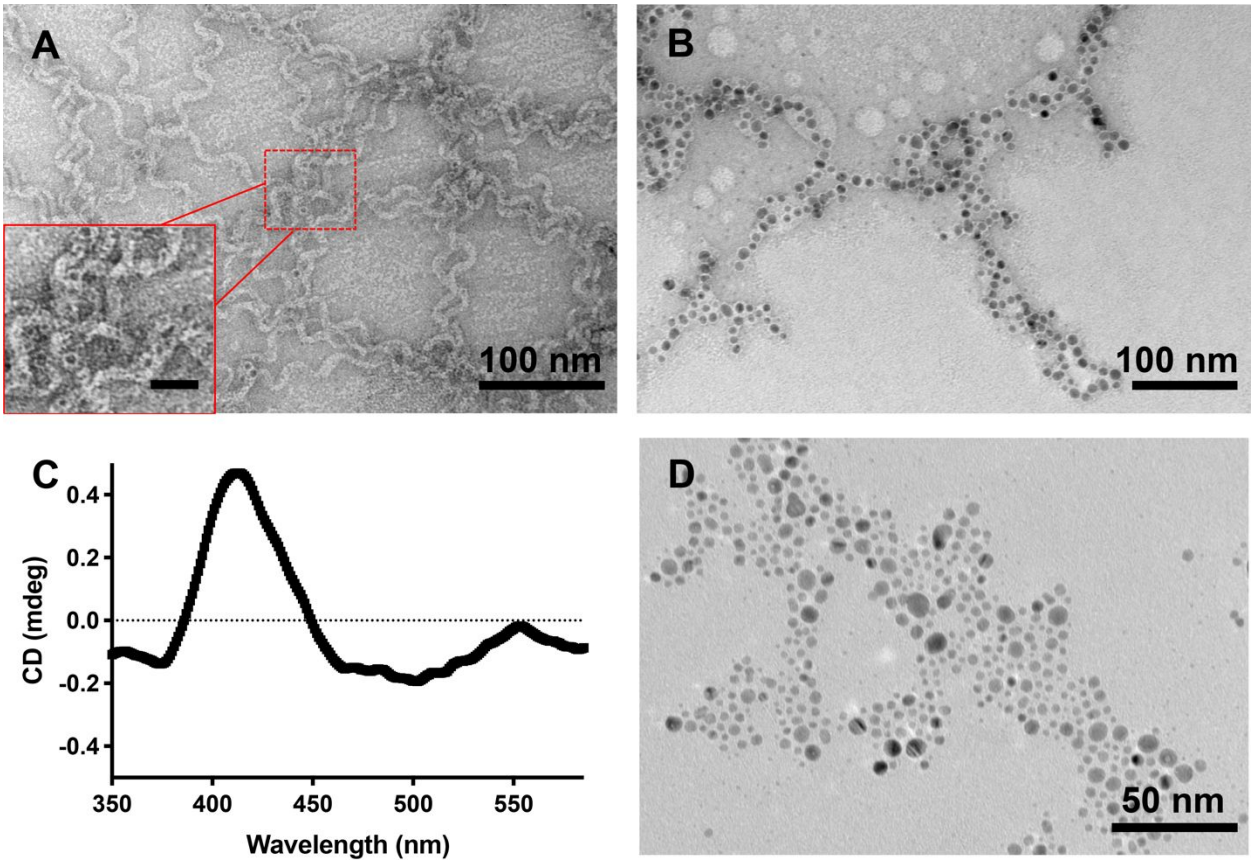

Figure S8. Representative TEM images of (A) AgSD/$\mathbf{K_S}\boldsymbol{C}\mathbf{'EK_S}$ without PSSS and (B) AgNP/$\mathbf{K_S}\boldsymbol{C}\mathbf{'EK_S}$ without PSSS grown from 200 μL seed solution. The insert in the bottom left corner of panel A shows a zoomed-in image of the areas outlined by the dashed red rectangle. The scale bar of the inset is 20 nm; (C) CD spectrum of AgNP/$\mathbf{K_S}\boldsymbol{C}\mathbf{'EK_S}$ w/o PSSS (nanoribbons); (D) A representative TEM image of pure AgNPs grown without an APA template.

Synthesis of pure Ag nanoparticles (AgNPs):

Preparation of pure AgNPs followed a previously published method.[12] In a 50 mL beaker, 10 mL of $AgNO_3$ solution (2 mM in water) was mixed with 1 mL of sodium citrate solution (2.5 mM in water), 0.5 mL PSSS solution (0.5 mg mL^{-1} in water), and 9 mL of Milli-Q water. Subsequently, 0.6 mL freshly prepared $NaBH_4$ solution (10 mM in ice-cold water) was added to the $AgNO_3$ solution. The color turned yellow upon addition of $NaBH_4$, indicating the formation of AgNPs.

Lyophilization stability:

2 mL of AgNP/$\mathbf{K_S}\boldsymbol{C}$'$\mathbf{EK_S}$, AgNP/$\boldsymbol{C}$'$\mathbf{EK_SK_S}$, AgNP/$\mathbf{K_S}\boldsymbol{C}$'$\mathbf{EK_S}$ without PSSS, and pure AgNPs were lyophilized to form a powder (FreeZone, -105 °C, Labconco, Kansas City, MO). After re-hydration in 2 mL DI water and vortexing for ~30 s, the absorbance of each sample from 250-800 nm was measured by a UV-Vis spectrometer (Agilent Cary 5000 spectrophotometer). During experiments, all the AgNP/APA hybrids and pure AgNPs were carefully collected from the cuvettes used for UV-Vis measurements through multiple rinses. With this procedure, the potential loss of AgNPs in each cycle is estimated to be <2%, which is negligible given the results of the study.

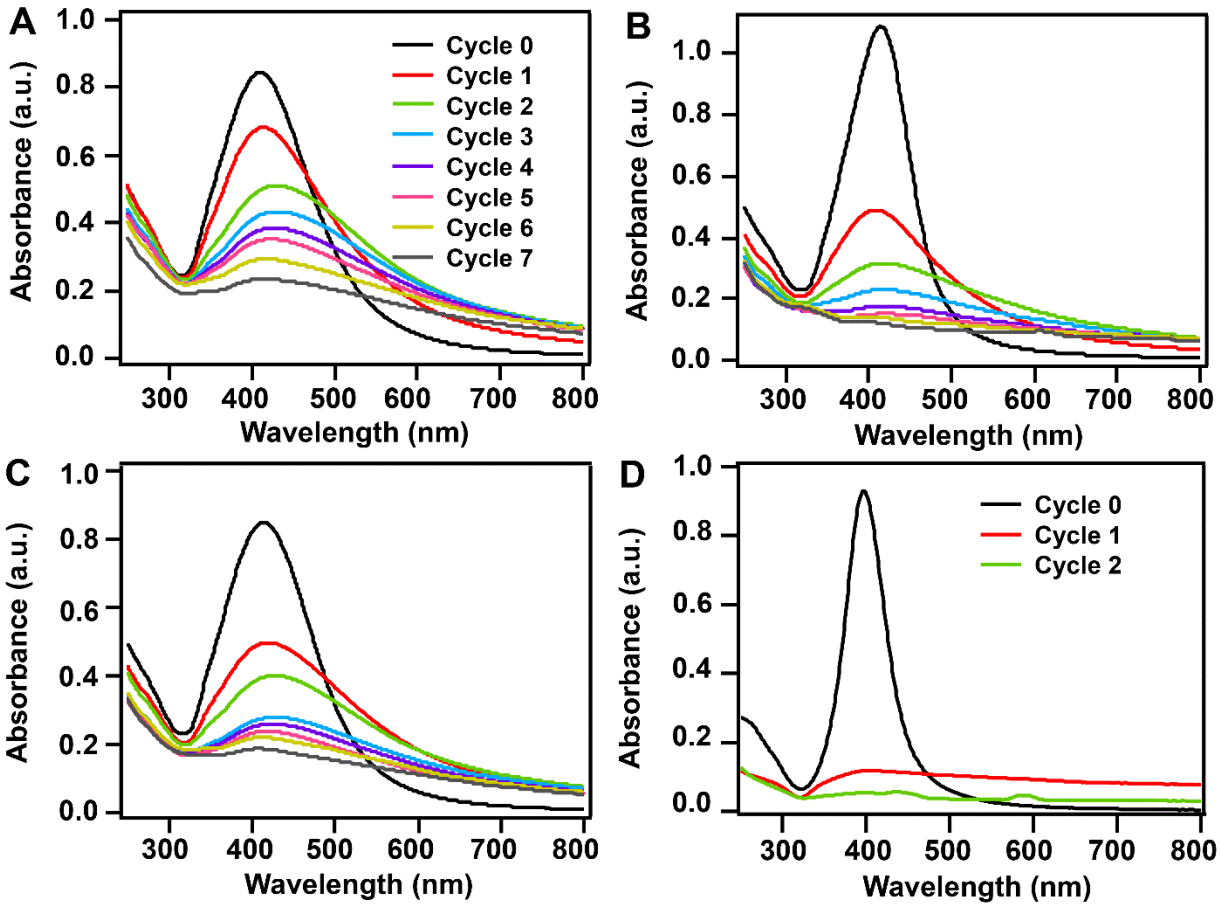

Figure S9. (A-D) UV-Vis spectra of (A) AgNP/$\mathbf{K_S}\boldsymbol{C}$'$\mathbf{EK_S}$, (B) AgNP/$\boldsymbol{C}$'$\mathbf{EK_SK_S}$, (C) AgNP/$\mathbf{K_S}\boldsymbol{C}$'$\mathbf{EK_S}$ without PSSS, and (D) pure AgNP solution after various lyophilization cycles. AgNP/$\mathbf{K_S}\boldsymbol{C}$'$\mathbf{EK_S}$ (A) showed the best viability upon lyophilization, and all AgNP/APA systems (A-C) showed improved stability against lyophilization compared to pure AgNP (D).

Data fitting equations used in Figure 3A:

AgNP/$\mathbf{K_S}\boldsymbol{C'}\mathbf{EK_S}$: $y = 0.242 + 0.765\exp(-0.382x)$

AgNP/ $\boldsymbol{C'}\mathbf{EK_SK_S}$: $y = 0.080 + 0.913\exp(-0.967x)$

AgNP/$\mathbf{K_S}\boldsymbol{C'}\mathbf{EK_S}$ w/o PSSS: $y = 0.255 + 0.735\exp(-0.726x)$

AgNP: $y = -0.001 + 1.000\exp(-2.704x)$

Colloidal stability against salt:

Solutions (0.5 mL) of AgNP/$\mathbf{K_S}\boldsymbol{C'}\mathbf{EK_S}$, AgNP/$\boldsymbol{C'}\mathbf{EK_SK_S}$, AgNP/$\mathbf{K_S}\boldsymbol{C'}\mathbf{EK_S}$ without PSSS, and pure AgNPs were mixed with 0.5 mL of phosphate buffer (pH 7.4) with different concentrations. The mixed solutions underwent vortexing for 30 s before collecting UV-Vis spectra (Agilent Cary 5000 spectrophotometer). The Ag^+ concentration for all samples was 114 μM.

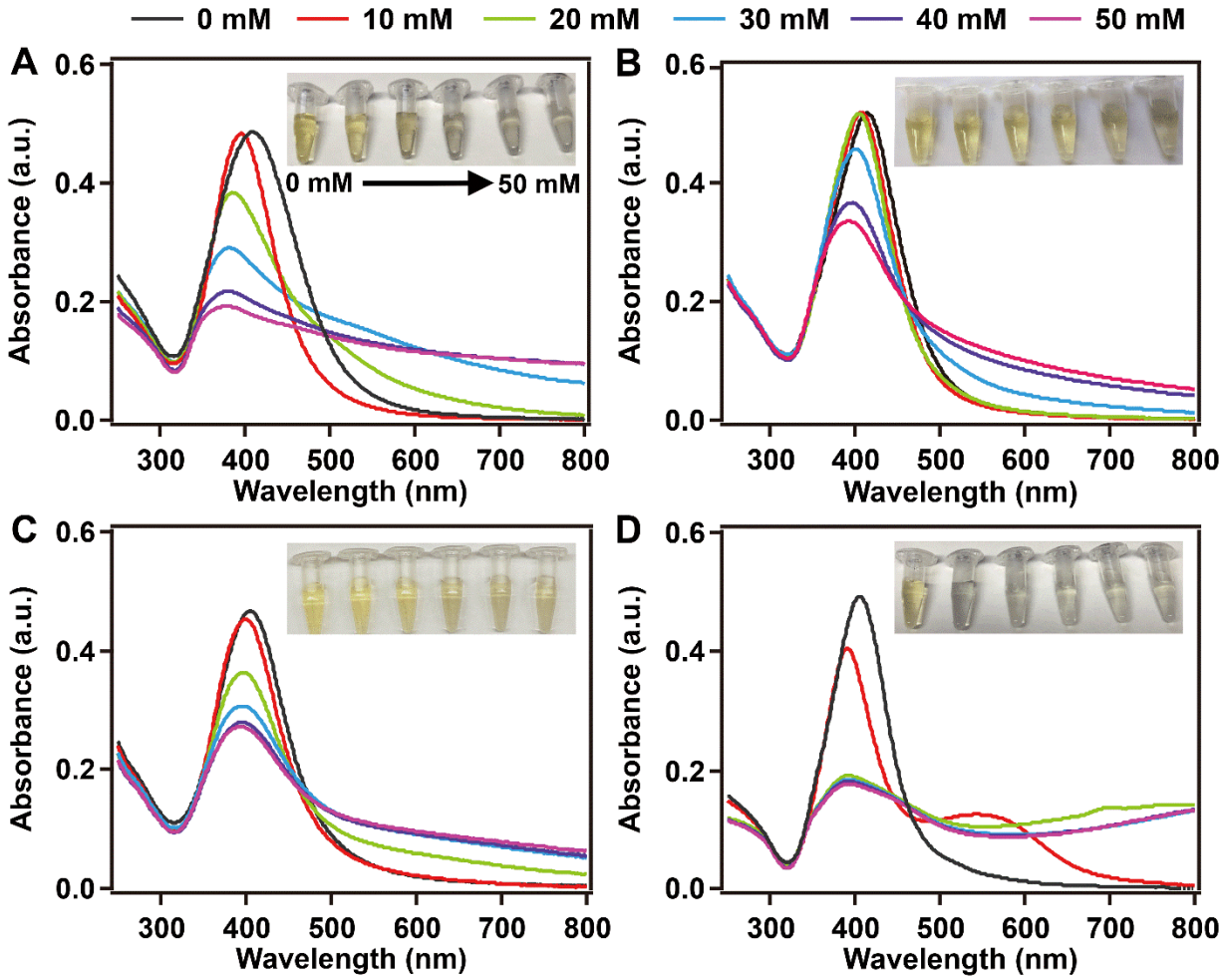

Figure S10. (A-D) UV-Vis spectra of (A) AgNP/$\mathbf{K_S}\boldsymbol{C'}\mathbf{EK_S}$, (B) AgNP/$\boldsymbol{C'}\mathbf{EK_SK_S}$, (C) AgNP/$\mathbf{K_S}\boldsymbol{C'}\mathbf{EK_S}$ without PSSS, and (D) pure AgNP solutions upon addition of PB with final concentrations ranging from 0 to 50 mM. Inset photographs show respective sample solutions after addition of PB.

Surface enhanced Raman spectroscopy:

Raman spectra were recorded by a WITec alpha 500 Raman spectrometer coupled with a confocal microscope (100× object lens) and a red laser (633 nm). The lateral size and power of the laser point were 0.3 μm and ~8 mW, respectively. The integration time and number of scans for spectra acquisition were 2 s and 40, respectively. Rhodamine B (RhB) and 2,2'-bipyridine (Bpy) were chosen as model Raman analytes. AgNP/APA solutions (AgNP/$\mathbf{K_SC'EK_S}$ and AgNP/$\mathbf{C'EK_SK_S}$) were mixed with RhB or Bpy solution (in water) to adjust the final concentration of the analytes to be 10^{-4} M. Afterward, 20 μL of each mixture was cast onto a piece of Al foil. The droplets were allowed to dry at room temperature and ambient pressure. Control experiments were carried out following the same protocol described above except using pure APA solution or pure AgNP solution. Each SERS measurement was repeated at least 3 times on each sample (each has three different spots), which accounts for a total of at least nine SERS spectra per group. A representative spectrum was chosen for each sample instead of averaging. Because SERS spectra are usually quite variable, and this variability by itself may contain some information about the sample, simple averaging can reduce this information significantly.

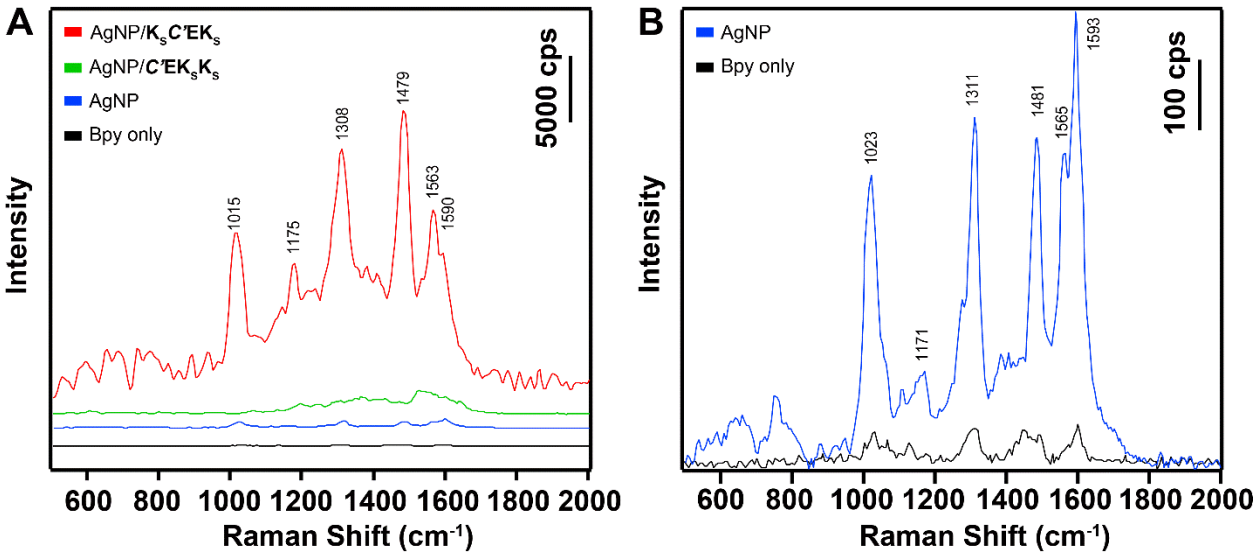

Figure S11. (A) SERS spectra of Bpy collected on AgNP/APA complexes with different morphologies, pure AgNP, and blank substrate (no enhancing materials). The concentration of Bpy for AgNP/APA complexes and pure AgNP was 10^{-4} M; it was 10^{-3} M for the blank substrate (Bpy only). (B) Magnified spectra of Bpy collected on pure AgNP (10^{-4} M Bpy) and blank substrate (10^{-3} M Bpy).

References

1. Foster, J. C.; Powell, C. R.; Radzinski, S. C.; Matson, J. B. *S*-aroylthiooximes: A facile route to hydrogen sulfide releasing compounds with structure-dependent release kinetics. *Org. Lett.* **2014**, *16*, 1558-1561.

2. Wang, Y.; Kaur, K.; Scannelli, S. J.; Bitton, R.; Matson, J. B. Self-assembled nanostructures regulate H_2S release from constitutionally isomeric peptides. *J. Am. Chem. Soc.* **2018**, *140*, 14945-14951.

3. Wang, Y.; Matson, J. B. Supramolecular nanostructures with tunable donor loading for controlled H_2S release. *ACS Appl. Bio Mater.* **2019**, *2*, 5093-5098.

4. Xing, Q. G.; Zhang, J. X.; Xie, Y. Y.; Wang, Y. F.; Qi, W.; Rao, H. J.; Su, R. X.; He, Z. M. Aromatic motifs dictate nanohelix handedness of tripeptides. *ACS Nano* **2018**, *12*, 12305-12314.

5. Gibb, B. C., Hofmeister's curse. *Nat. Chem.* **2019**, *11*, 963-965.

6. Pashuck, E. T.; Stupp, S. I. Direct observation of morphological tranformation from twisted ribbons into helical ribbons. *J. Am. Chem. Soc.* **2010**, *132*, 8819-8821.

7. Kumar, C. V.; Buranaprapuk, A. Tuning the selectivity of protein photocleavage: Spectroscopic and photochemical studies. *J. Am. Chem. Soc.* **1999**, *121*, 4262-4270.

8. Goldhahn, C.; Schubert, J.; Schlaad, H.; Ferri, J. K.; Fery, A.; Chanana, M. Synthesis of metal@protein@polymer nanoparticles with distinct interfacial and phase transfer behavior. *Chem. Mater.* **2018**, *30*, 6717-6727.

9. Sangwai, A. V.; Sureshkumar, R. Coarse-grained molecular dynamics simulations of the sphere to rod transition in surfactant micelles. *Langmuir* **2011**, *27*, 6628-6638.

10. Feng, J.; Wong, K. Y.; Lynch, G. C.; Gao, X. L.; Pettitt, B. M. Salt effects on surface-tethered peptides in solution. *J. Phys. Chem. B* **2009**, *113*, 9472-9478.

11. Jelesarov, I.; Durr, E.; Thomas, R. M.; Bosshard, H. R. Salt effects on hydrophobic interaction and charge screening in the folding of a negatively charged peptide to a coiled coil (leucine zipper). *Biochemistry* **1998**, *37*, 7539-7550.

12. Aherne, D.; Ledwith, D. M.; Gara, M.; Kelly, J. M. Optical properties and growth aspects of silver nanoprisms produced by a highly reproducible and rapid synthesis at room temperature. *Adv. Funct. Mater.* **2008**, *18*, 2005-2016.